Title

A bioavailable strontium isoscape of Angola with implications for the archaeology of the transatlantic slave trade

Authors

Wang, Xueye

Bocksberger, Gaëlle

Lautenschläger, Thea

et al.

Publication Date

2023-06-01

DOI

10.1016/j.jas.2023.105775

Peer reviewed

Journal of Archaeological Science 154 (2023) 105775

Contents lists available at ScienceDirect

Journal of Archaeological Science

journal homepage: www.elsevier.com/locate/jas

A bioavailable strontium isoscape of Angola with implications for the archaeology of the transatlantic slave trade

Xueye Wang [a], Gaëlle Bocksberger [a], Thea Lautenschläger [b], Manfred Finckh [c], Paulina Meller [c], Gregory E. O'Malley [d], Vicky M. Oelze [a,*]

[a] Anthropology Department, University of California Santa Cruz, 1156 High Street, CA, 95064, Santa Cruz, USA
[b] Department of Biology, Institute of Botany, Faculty of Science, Technische Universität Dresden, 01062, Dresden, Germany
[c] Department of Biology, Institute of Plant Science and Microbiology Biodiversity, Evolution and Ecology, Hamburg University, Ohnhorststr. 18, 22609, Hamburg, Germany
[d] History Department, University of California Santa Cruz, 1156 High Street, CA, 95064, Santa Cruz, USA

ARTICLE INFO

Keywords:
strontium isotope analysis
random forest regression
forced migration
African Diaspora
archaeological mobility

ABSTRACT

The region of present-day Angola was one of the main areas from which millions of enslaved Africans were abducted and forced to migrate to the Americas during the transatlantic slave trade. Strontium isotope ($^{87}Sr/^{86}Sr$) analysis is a useful tool in reconstructing large-scale human movements across geologically distinct landscapes in archaeological and forensic contexts. However, the absence of environmental $^{87}Sr/^{86}Sr$ reference data from Angola hinders the use of $^{87}Sr/^{86}Sr$ analysis in provenance studies related to Angola, especially in identifying the geographic origin of enslaved people in the African Diaspora. Here, we measured 101 plant samples from most, yet not all, major geological units to draft the first bioavailable $^{87}Sr/^{86}Sr$ map (isoscape) for Angola using a machine learning framework. Our results suggest that the $^{87}Sr/^{86}Sr$ ratios in Angola span a large range from 0.70679 to 0.76815 between the different geological units. Specifically, the high average $^{87}Sr/^{86}Sr$ ratios of 0.74097 (±0.00938, 1 SD) found in the Angola Block of central Angola, are distinctly more radiogenic than any previously published bioavailable $^{87}Sr/^{86}Sr$ ratios for western Central and West Africa. However, these match the $^{87}Sr/^{86}Sr$ ratios previously published for human enamel samples from four historic slavery contexts in the Americas. We demonstrate that our strontium isoscape of Angola greatly improves the ability to assess the possible origins of enslaved African individuals discovered outside of Africa and encourage the future use of emerging African isoscapes in the study of life histories within the slave trade.

1. Introduction

1.1. Angola – prehistoric archaeology and historic background

Located in an ecological transition zone between the Congo Basin and Namib Desert along the South Atlantic Ocean, Angola is a key region for studying early human adaptations and evolution in Southwestern Africa (summarized in de Matos and Pereira, 2020). Since the 1940s, hundreds of Paleolithic sites have been discovered in this region, including tens of thousands of pre-Acheulean to Late Stone Age lithic artifacts and a rich faunal fossil record dating from the late Pliocene to the Holocene era (e.g. Gilbert et al., 2009; de Matos, 2015; Lebatard et al., 2019; de Matos et al., 2021; de Matos and Pereira 2020). Although Angola has a rich and unique prehistoric and historic past, archaeological research rapidly declined with the long battle for independence from Portugal and the brutal civil war which grasped the country between 1975 and 2002. Investments into Angolan archaeology were slow to pick up again in times of peace because of the war's many legacies such as the abundance of land mines and the loss of museum collections and academic infrastructure (de Matos et al., 2021).

One particularly difficult chapter of Angola's history is without a doubt the time of the transatlantic slave trade. Angola was one of the most important regions supplying enslaved Africans for the Americas, with more than 3.5 million African individuals estimated to have embarked from the region's two principal ports, Luanda and Benguela, between the 16th and 19th centuries (Miller, 1988; Eltis and Richardson, 2010; Domingues da Silva, 2013). Most of these captives endured the Middle Passage aboard Portuguese (or Brazilian) ships, bound for the

* Corresponding author.
E-mail address: voelze@ucsc.edu (V.M. Oelze).

https://doi.org/10.1016/j.jas.2023.105775
Received 27 October 2022; Received in revised form 30 March 2023; Accepted 4 April 2023
Available online 13 April 2023

Portuguese colony of Brazil, or to a lesser degree, the colonies of Spanish America, since Portuguese and Brazilian traders were important suppliers of enslaved people to Spanish America (Eltis and Richardson, 2010; Borucki et al., 2015).

Although the prominence of Angolan ports in the Atlantic slave trade is well established, the origins of captives who embarked at any particular African port are a matter of debate among historians. While some written records of European traders documented the seaborne movements of individual ships and broader patterns in the maritime portion of the slave trade, records on trafficking of people within Africa before reaching the coasts are scarce. One particular debate engaging historians studying many parts of West and West Central Africa regards the reach of the Atlantic slave trade into the interior, with some scholars emphasizing the deeper penetration of slaving zones into the interior as the scale of the Atlantic trade grew (Lovejoy and Richardson, 1995; Thornton, 1998; Lovejoy, 2012), while others argue that enslavement within a few hundred miles of the coast always supplied most captives to European traffickers (Manning, 1982). Historians of the Angolan slave trade have engaged in particular version of this debate, with some scholars emphasizing an expanding frontier of enslavement with Portuguese raiders making inland incursions from Luanda and especially the expansion of slave raiding African states in the interior as the Atlantic trade grew (Miller, 1988; Lovejoy, 2012). Recent scholarship, however, questions this emphasis on eastward migration of the slaving zones through warfare, arguing that enslavement did not only occur on the violent margins of eastward-expanding states, but also through criminal prosecutions and adjudication of defaulted debts within states closer to the coast (Domingues da Silva, 2013).

Overall, historians are more confident in their mapping of the ports and routes of the transatlantic portion of the slave trade than they are in identifying the precise ethnic, linguistic, or geographic origins of enslaved people (Trans-Atlantic Slave Trade Database, 2022). The anonymous nature of European trade records that treated enslaved people as commodities, very rarely recording their names or backgrounds. This limits historians' abilities in tracing individual stories. Strontium isotope analysis in human remains from New World burial sites associated with slavery thus holds great potential to shed light on two aspects of the slave trade that historians struggle to see—the particular origins of enslaved people within Angola and the particular journeys of specific individuals within this broader forced migration. These advantages make this method a valuable tool, increasingly utilized in investigations of the transatlantic slave trade (Price et al., 2006, 2012; Schroeder et al., 2009, 2014; Bastos et al., 2016; Fleskes et al., 2021).

1.2. Isotopes, isoscapes and investigations of the slave trade

The $^{87}Sr/^{86}Sr$ analysis has been widely applied to identify home ranges and movements of human and animals in archaeology (Ericson, 1985; Slovak and Paytan, 2012). The principle is that variation in $^{87}Sr/^{86}Sr$ is primarily linked the ratio of rubidium (Rb) to strontium (Sr) as well as the age of a given bedrock (Bentley, 2006, see details in supplementary text). A bedrock's $^{87}Sr/^{86}Sr$ composition, is weathered into the soil where it is taken up by plants, which pass a location's $^{87}Sr/^{86}Sr$ ratio on to consumers. Ultimately, these $^{87}Sr/^{86}Sr$ ratios are incorporated into body tissues of animals (e.g. bioapatite like teeth and bones) as they form, where Sr substitutes for calcium (Bentley, 2006). Previous studies showed that the bioavailable $^{87}Sr/^{86}Sr$ ratios in plants can differ from the ratio in bedrock and whole soils (Sillen et al., 1998; reviewed in Price et al., 2002) due to various environmental factors such as differential weathering of mineral components or Sr inputs from atmospheric sources (reviewed in Bataille et al., 2020; Crowley et al., 2017). Therefore, archaeologists primarily measure bioavailable $^{87}Sr/^{86}Sr$ ratios in organic materials when determining a location's bioavailable $^{87}Sr/^{86}Sr$ variation.

Using $^{87}Sr/^{86}Sr$ analysis in reconstructing the geological origins of individuals requires information on the $^{87}Sr/^{86}Sr$ variation in a landscape, a so called *isoscape*. To date, several projects used environmental samples (e.g. plants, soil leachates and low-mobility animals) and different modeling approaches (e.g. geostatistical spatial interpolation models) to develop large-scale strontium isoscapes (e.g. Bataille et al., 2020; Wang and Tang, 2020). Recently, researchers started using machine learning methods such as random forest regression (Bataille et al., 2018; Hoogewerff et al., 2019), which combine observed $^{87}Sr/^{86}Sr$ data and important environmental auxiliary predictors, which largely improved the predictive power of isoscapes for Europe (Bataille et al., 2018), Kenya and northern Tanzania (Janzen et al., 2020), and even at the global scale (Bataille et al., 2020). However, the accuracy of these models is still highly dependent on the availability of environmental $^{87}Sr/^{86}Sr$ data itself (Bataille et al., 2020). Particularly in Africa, the performances of models are extremely poor due to low data coverage (Bataille et al., 2020; Janzen et al., 2020). The need for environmental $^{87}Sr/^{86}Sr$ data from Africa appears particularly relevant ever since $^{87}Sr/^{86}Sr$ data has been obtained from skeletal remains of enslaved Africans in the New World, particularly in the Caribbean (Schroeder et al., 2009, 2014; Laffoon et al., 2018; Fricke et al., 2021), Brazil (Bastos et al., 2016), and North America (Goodman et al., 2004; Price et al., 2006, 2012; Barquera et al., 2020; Quinn et al., 2020; Smith-Guzmán et al., 2020). Many of these studies found considerable $^{87}Sr/^{86}Sr$ variation among enslaved individuals, suggesting that these people were of diverse geological origins and several had been exposed to particularly radiogenic $^{87}Sr/^{86}Sr$ ratios in their environment during tooth formation. Some of these individuals showed radiogenic $^{87}Sr/^{86}Sr$ ratios higher than 0.730, which exceed what has been reported for Sr isoscapes within in the Americas (e.g. United States, Dutch Caribbean and Mexico), suggesting these persons grew up in regions with particularly ancient and highly radiogenic bedrock, presumably sub-Saharan Africa (Price et al., 2006, 2012; Schroeder et al., 2014; Bastos et al., 2016; Fleskes et al., 2021). These studies provided convincing evidence of potential first-generation captives from Africa and hence new insights into the individual migration histories of enslaved Africans. However, due to the lack of bioavailable Sr isoscapes for the largest parts of Africa, past research could not assess regional African origins based on $^{87}Sr/^{86}Sr$ results but relied on historical documents or cultural markers such as dental modifications to speculate about the potential origins of individuals from so-called slave cemeteries.

In the case of Angola, the absence of environmental $^{87}Sr/^{86}Sr$ reference data hinders the use of $^{87}Sr/^{86}Sr$ analysis in bioarchaeological investigations and limits our ability to identify the countless enslaved individuals who must have had roots in Angola. We here argue that the geology of Angola with its Archean basement rocks in the center the country is an ideal region in West and western Central Africa to detect characteristically high $^{87}Sr/^{86}Sr$ ratios and associate them with individuals from New World slavery context with particularly high $^{87}Sr/^{86}Sr$ ratios. In this study, we measured the $^{87}Sr/^{86}Sr$ ratios of modern plants collected along transects across Angola and employed a random forest regression modeling approach to create the first bioavailable $^{87}Sr/^{86}Sr$ map of Angola. We use this isoscape to explore the potential geographical origins of selected individuals from the previous bioarchaeological studies mentioned above.

2. Materials and methods

2.1. Geological background

Angola is located on the western Atlantic Coast of Southern Africa between ~18°S and ~4°30′S. The topography of Angola is relatively diverse, including coastal basins, and low plains and terraces north of 10°S with an average elevation of 500 m, as well as mountains and central plateau south of 10°S. Located on the Atlantic coast between the Tropic of Capricorn and the Equator, Angola harbors a hyper-arid climate in the south and hyper-humid climate in the north (Dinis

et al., 2017).

Overall, the geology of Angola is characterized by the Mesozoic-Cenozoic sediments in the east and the Precambrian rocks in the west (Fig. 1). North of ~10°S latitude, the West Congo Belt consists of the unmetamorphosed Neoproterozoic strata in the east, Pan-African Belts (~650-550 Ma) in the middle and reworked Precambrian basements in the east (Dinis et al., 2017). South of ~10° S latitude, the region is dominated by the Angola Block in the west and broad Mesozoic-Cenozoic sedimentary cover in the east. The core of the Angola Block is represented by widespread felsic Eburnean (~2 Ga) plutonic and metamorphic rocks (De Waele et al., 2008; Dinis et al., 2017). The southeastern margin of the Angola Block is composed of large mafic intrusions of the Mesoproterozoic Cunene Intrusive Complex, while the northeastern margin is the Liberian-Limpopo massif which consist of Neoarchean granites, gneisses and migmatites occurring together with mafic complexes and carbonatite (De Carvalho et al., 2000; Bambi et al., 2012; Garzanti et al., 2018). Along the Atlantic margin of Angola, the Precambrian bedrock is covered by mostly Mesozoic-Cenozoic sediments with the thickness of several kilometers (Chaboureau et al., 2013). In eastern Angola, the hinterland is covered by Meso-Cenozoic fluvial and aeolian sediments, which are part of the Kalahari sequence stretching 2200 km from South Africa to the Congo (Haddon and McCarthy, 2005; Dinis et al., 2017).

2.2. Sample collection

We sampled a total of 101 modern plants from 99 different sites along systematic botanical transects conducted between 2011 and 2021. Plant samples from the Herbarium Dresdense were obtained under a long-term cooperation agreement between TU Dresden (Germany) and the *Instituto Nacional da Biodiversidade a Areas de Conservação* (INBAC). Export permits (#01/018, #03/018, #06/2019, #012/2015, #1/2015, and #166/2016) were granted by the *Direcção Provincial da Agricultura, Pecuária e Pescas* of Uíge Province and Cuanza Norte Province (Angola) in collaboration with the *Universidade Kimpa Vita* (Angola). Plant samples from the Herbarium Hamburgense were obtained through scientific cooperation of Universität Hamburg with the *Instituto Superior de Ciencias de Educaäo da Huila* (ISCED-Huila) in the context of The Future Okavango (TFO) and SASSCAL projects. Export permits were provided by the National Directorate of Agriculture, Lifestock and Forest (Angola) under Material Transfer Agreements #20120907, #20150312, 20,160,525, 20,170,605, #20200623 and #12/13 between ISCED-Huila in Angola and Hamburg University in Germany. Plant import from Germany to the United States for analysis was granted by the USDA under permit #PCIP-21-00070.

Our sampling strategy focused on covering all geological units with 2–3 different sampling locations (habitat plots) at which we selected several different plant types (e.g., different types of herbaceous vegetation, shrubs, trees, and climbers) with presumably very different rooting depths. Though root morphologies for most of these plants are not described, we assume that most shrubs and trees have relatively deep root systems as they are adapted to seasonal dry conditions, whereas terrestrial vegetation (perineal and annual herbs and grasses) have much more shallow root systems as we recovered most of these during sampling (see Table S1). We were not able to cover geological units in the south-eastern provinces of Cuando Cubango and Moxico, as well as the more Namib Desert influenced province of Namibe. However, as these regions have very low population densities of below 5 inhabitants/km^2 we feel confident that the lack of sample coverage and hence isoscape accuracy in these regions is acceptable for an isoscape primarily drafted to model human origins during the slave trade.

All habitat plots were located away from settlements, roads and farmland to avoid potential anthropogenic Sr contaminations (e.g. from traffic, fertilizers or pesticides) and georeferenced using hand-held GPS devices with accuracy of ±10 m. Plants were identified to species or genus level and prepared for the two herbarium archives Herbarium Dresdense (TU Dresden) and Herbarium Hamburgense (Hamburg University) by dry pressing in the field and subsequent dry storage. From each herbarium specimen, 1–2 g of dry leaves and/or stems were selected for $^{87}Sr/^{86}Sr$ analysis.

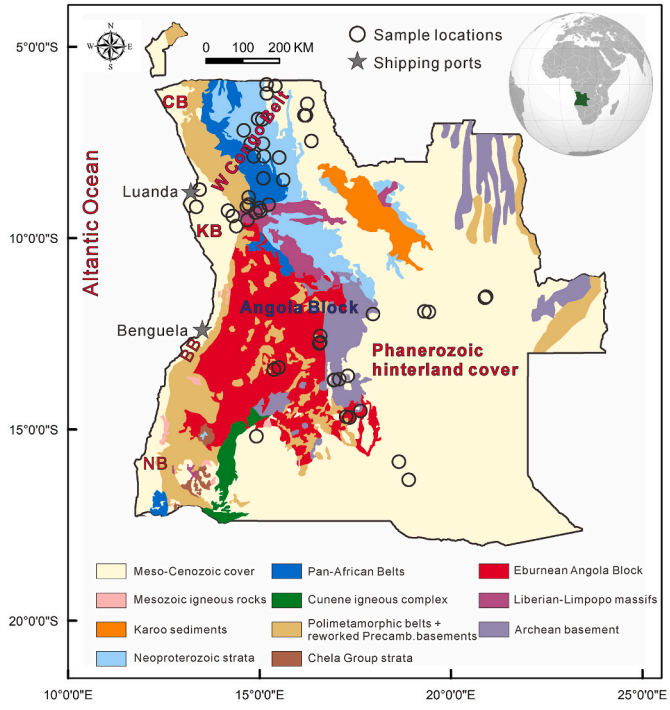

Fig. 1. Plant sampling locations in this study and the geological map of Angola modified after Garzanti et al. (2018) and Dinis et al. (2017) (CB: Congo Basin; KB: Cuanza Basin; BB: Benguela Basin; NB: Namibe Basin).

2.3. Isotope analysis

We followed standard sample preparation and measurement procedures for strontium isotope analysis of organic materials (Copeland et al., 2008; Deniel and Pin, 2001). The dried plants were ashed in a muffle furnace at 800 °C for 12 h in the Primate Ecology and Molecular Anthropology Lab at UCSC. For Sr separation and isotopic measurement, samples were transferred to the clean lab facilities at the UCSC W.M. Keck Isotope Laboratory. To separate strontium we followed the ion exchange method outlined by (Deniel and Pin, 2001). Each ashed plant was digested in 2 ml of 65% HNO_3 on a hot plate set to 120 °C for 2 h. The supernatant was dried and re-dissolved in 1 ml of 3 N HNO_3. The Sr fraction was separated from the samples using Eichrom Sr-Spec resin (50–100 μm). Sr isotopic ratio measurements were conducted using the IsotopX X62 Phoenix Thermal Ionization Mass Spectrometer (TIMS). The $^{87}Sr/^{86}Sr$ measurements were corrected for mass fractionation and normalized to $^{86}Sr/^{88}Sr = 0.11940$. The NIST SRM-987 standard was analyzed during measurement and yielded a mean $^{87}Sr/^{86}Sr$ ratio of 0.710239 ± 0.000017 (2σ, n = 13), in agreement with the SRM-987 standard value of 0.710250. Procedural blanks prepared with every batch of 19 samples were measured via an Element XR High Resolution ICP-MS system in the UCSC Plasma Lab and consistently yielded lower Sr concentrations than 200 pg.

2.4. Isoscape modeling approach

We used a random forest algorithm to model bioavailable $^{87}Sr/^{86}Sr$ ratios and predicted an isoscape of Angola. Random forest (RF) regression is an ensemble-based machine learning approach implemented by averaging deep decision trees and using bagging (bootstrap sampling of the training data) to reduce the variance of the model (Breiman, 2001).

Its higher predictive power compared to other geostatistical or regression methods makes it a powerful method to generate Sr isoscapes (Bataille et al., 2020; Serna et al., 2020; Kramer et al., 2022).

As potential predictors, we first chose a series of 31 independent variables, including geological, climatic, topographic, and environmental variables (Table S2). Some of the predictor rasters were provided by Bataille et al. (2020) in the equal-area Eckert IV projection with a grid cell size of 1 km^2, others we compiled ourselves from multiple sources with the same resolution and projection. Although RF is known to handle high-dimensional data well, correlation and collinearity between predictors can result in poor permutation importance and complicate interpretation (Gregorutti et al., 2017). In order to inform our selection of the most valuable predictors for our dataset, we used a mix of methods: 1) a three step selection using RF (Genuer et al., 2019), 2) reduction of multicollinearity with Pearson's correlation and variance inflation factor (Benito, 2021), and 3) visual inspection of the predictor's correlation. This selection process informed our decision to finally select 7 predictors (Table 1). We first optimized two of the model hyperparameters (number of variables randomly sampled at each split and maximum node size). Then the RF model was trained with the full sample set and k-fold cross validation approach (5 partitions, repeated 10 times). We used the mean R^2 and RMSE of the error predictions as model accuracy. The importance of each predictor was calculated by averaging the difference of predictive accuracy of each tree when a predictor is randomly permuted (permutation importance, Wright et al., 2016). We computed the partial dependence of the response to each predictor to evaluate the relationships between the selected covariate and the observed values. We also checked the linear fit between predicted and observed data, as well as the distribution of the residuals, to assess the model predictive ability. Finally, we used the model to predict a Sr isoscape of Angola.

For comparisons with our RF modeling results, we used an ordinary kriging interpolation method which depends on statistical models of spatial autocorrelation to generate a baseline map for Angola. The kriging map was created using ESRI ArcMAP 10.2. Additionally, we checked the accuracy of a previously published global isoscape that included estimates for Angola (Bataille et al., 2020), by comparing the previous modeled isoscape with our novel isoscape based on locally observed isotopic data. Please see supplementary materials for the software used.

2.5. Assignment of human $^{87}Sr/^{86}Sr$ ratios to Angola

We considered previously published human enamel $^{87}Sr/^{86}Sr$ data from four slave cemeteries that contained individuals with distinctively high $^{87}Sr/^{86}Sr$ ratios (>0.730) to test the potential of our novel isoscape. These included individuals from the 18th to 19th century (1769–1830 CE) burial site of Pretos Novos located in Rio de Janeiro, Brazil (n = 30, Bastos et al., 2016), the mid to late 17th-century cemetery in the Zoutsteeg area of Philipsburg in the Dutch Caribbean (n = 3; Schroeder et al., 2014), burials from the 16th to 17th century early colonial church in Campeche, Mexico (n = 112; Price et al., 2006, 2012), as well as the 18th-century Anson Street African Burial Ground, Charleston, USA (n = 29; Fleskes et al., 2021).

To showcase the potential of isoscapes in determining the potential geological/geographic origins of individual human beings, we calculated the posterior probability of origin of four representative individuals selected from these four burial sites using our Angolan isoscape. We selected one individual per site, with a focus on different $^{87}Sr/^{86}Sr$ ratios higher than 0.730 (Anson Street African Burial Ground: 0.73076; Pretos Novos cemetery: 0.74985; Zoutsteeg area of Philipsburg: 0.73433; Campeche cemetery: 0.73912). The isotope ratios of these four individuals cover different isotopic ranges we describe for Angola and are considered rare for most other parts of the world. Probability surfaces of each individual are normalized to highlight the probability of origin of each $^{87}Sr/^{86}Sr$ ratio. Please see supplementary materials for the software used.

3. Results and discussion

3.1. Bioavailable $^{87}Sr/^{86}Sr$ ratios in plants

The $^{87}Sr/^{86}Sr$ ratios collected from 101 plant samples range from 0.70679 to 0.76815, with a high mean of 0.72829 ± 0.01076 (1 SD), generally reflecting the heterogeneous geological characteristics of Angola. Overall, the distribution of the bioavailable $^{87}Sr/^{86}Sr$ dataset is relatively asymmetric (kurtosis = 1.23 and skewness = 0.71), with a Shapiro–Wilk test indicating that the dataset is non-normally distributed ($p < 0.05$). Most of the isotopic composition (60%) ranges between 0.720 and 0.735, 16% data are distributed in the lower interval between 0.706 and 0.720, and 24% of the dataset is represented by high ratios ranging from 0.735 to 0.768 (Fig. S1). The most radiogenic ratio is found in the Eburean Angola Block in southern Angola and the lowest radiogenic ratio comes from the West Congo belt in northern Angola. Overall, $^{87}Sr/^{86}Sr$ ratios show large variability in different geological units and display a strong north-south gradient with increasing ratios from the West Congo Belt ($\bar{x}$ ± SD: 0.72438 ± 0.00773, n = 26) and west Limpopo-Liberian Massifs ($\bar{x}$ ± SD: 0.71209 ± 0.05601, n = 6) to the Angola Block ($\bar{x}$ ± SD: 0.74097 ± 0.00938, n = 22) (see details in supplementary text and Fig. S2).

Overall, Angola presents more radiogenic and highly distinctive bioavailable $^{87}Sr/^{86}Sr$ ratios (>0.730) than other regions in West and western Central Africa and coastal East Africa based on the published bioavailable $^{87}Sr/^{86}Sr$ data, including Ghana (0.7234–0.7296; Goodman et al., 2004), Nigeria (0.7074–0.7165; Pye, 2004), Cameroon (0.7089–0.7193; Viers et al., 2000), Namibia (0.7206–0.7282; Vogel et al., 1990), Congo River Basin (0.7155–0.7277; Palmer and Edmond, 1989; Négrel et al., 1993; Allègre et al., 1996), and Mozambique (0.7206–0.7247; Dominy et al., 2020). We are aware of a small region with slightly higher $^{87}Sr/^{86}Sr$ ratios in western Côte d'Ivoire, southern Ghana, eastern Liberia and Guinea yet this data is not yet published (Wang et al. in prep.). Considerably higher $^{87}Sr/^{86}Sr$ ratios than what we here report for Angola, are so far only published for South Africa (Copeland et al., 2011; Fowler et al., 2020) and parts of Zimbabwe (House et al., 2021).

Table 1
List of geological, climatic, topographic and environmental variables used in the predicted model. Resolution and object type describe the published data (P = Polygon; R = Raster). To be used in the analyses, the published data was resampled into rasters with 1 km × 1 km resolution and an equal area projection.

Variables names in R script	Description	Resolution	Object type	Source
geol_agemax	Maximum age attribute from African geological map (myrs)	1:10 million	P	Thiéblement et al. (2016)
ai_reproj	Global aridity index	30-arc sec	R	Zomer et al. (2008)
basement_age_reproj	Terrane age attribute (myrs)	5° × 5°	R	Mooney et al. (1998)
elevation_reproj	SRTM (m)	90 m	R	Jarvis et al. (2008)
rcec_reproj	Soil cation exchange capacity	250 m	R	Hengl et al. (2017)
rclay_reproj	Soil clay content (weight %)	250 m	R	Hengl et al. (2017)
orc	Soil organic carbon content (weight %)	250 m	R	Hengl et al. (2017)

3.2. A $^{87}Sr/^{86}Sr$ isoscape of Angola based on random forest regression

The random forest regression model allowed us to draft the first bioavailable $^{87}Sr/^{86}Sr$ map for Angola based on local samples (Figs. 2 and 3, and see high resolution images via Mendeley Data: https://doi.org/10.17632/b4tp235xp6.1). The random forest model accounts for 66% of the variation, showing an average cross-validation root-mean-square error (RMSE) of 0.0065 ± 0.0012 over the dataset, while the residuals range from −0.018 – 0.028 (64% fall between ± 0.005) (Fig. 3B and C). The standard prediction errors are mostly within 0.004, with some higher errors (up to 0.008) in southeastern Angola due to low sampling density (Fig. S3). Although the RMSE in this study is higher compared to that of other regions using similar predictors (e.g. northern Tanzania and southern Andes; Janzen et al., 2020; Barberena et al., 2021), it actually only represents about 11% of the whole $^{87}Sr/^{86}Sr$ dataset range over the study area as Angola has much more variable $^{87}Sr/^{86}Sr$ ratios than those regions. Overall, our model shows adequate predictive power to generate a $^{87}Sr/^{86}Sr$ map for Angola.

Informed by the results of variable selection and observation of correlation and collinearity, as well as our expert knowledge, we selected 7 predictive variables, including elevation, soil characteristics, climate, and geological variables. Among them, the variables elevation, soil organic carbon content, and soil clay content have the highest predictive power (Fig. 3A). From the partial dependence plots (Fig. S4), it is clear that $^{87}Sr/^{86}Sr$ ratios increase nearly linearly with increasing elevation. This is because the subaerial exposure of Precambrian granites dominated in the Angola Block may provide higher $^{87}Sr/^{86}Sr$ weatherable minerals during tectonic uplift (Capo et al., 1998). In high relief areas, increased physical erosion can accelerate the weathering rate of the old felsic rocks (Bentley, 2006), possibly causing more radiogenic $^{87}Sr/^{86}Sr$ ratios in the mountain and plateau regions of the Angola Block. Other factors, including aridity index and soil characteristics (clay content, organic carbon content, and cation exchange capacity), show non-linear relationships with the $^{87}Sr/^{86}Sr$ ratios.

Geological variables (terrane age and maximum age of rocks) present very low variable importance scores of all selected predictors. This could be because 1) the current available GLiM database has very low spatial resolution for Africa with relevant geological information only available for large-scale geological units (Hartmann and Moosdorf, 2012); and 2) the Rb/Sr contents and ages of igneous, metamorphic and sedimentary rocks are highly variable in nature (Hajj et al., 2017), which could result in poor predictive power of these geological variables in mapping the old Precambrian basement regions (as it experienced a series of tectonic, metamorphic, and magmatic events), such as the case for Angola (De Carvalho et al., 2000). Notely, the bioavailable $^{87}Sr/^{86}Sr$ distribution in Angola shows distinct patterns in different geological units (Fig. S2), indicating that geological factors that cannot be ignored which we thus incorporated in the model. Soil factors are also included into the model because soils are weathered from parent rocks and, in another perspective, soil properties can inherit local geological features and be influenced by local climatic conditions as well (Capo et al., 1998).

3.3. Comparing different isoscape models

To further evaluate the prediction of our modeling, we used the ordinary kriging interpolation method to model the Sr isoscape as well as cropped Angola out of the global isoscape established by Bataille et al. (2020) for comparison (Fig. 4). Overall, the ordinary kriging produced a very similar R^2 and RMSE with the RF model shown in this study (R^2 = 0.66, RMSE = 0.0062). However, although displaying similar spatial $^{87}Sr/^{86}Sr$ distributions, the kriging approach is more likely to overfit the data and therefore lead to the loss of $^{87}Sr/^{86}Sr$ heterogeneity at the local scale (Fig. 4C) (Lugli et al., 2022). Additionally, the kriging interpolation is based on spatial autocorrelation without taking any $^{87}Sr/^{86}Sr$ influencing environmental factors into consideration. Consequently, the kriging modeling result tends to create unreliable maps in areas without

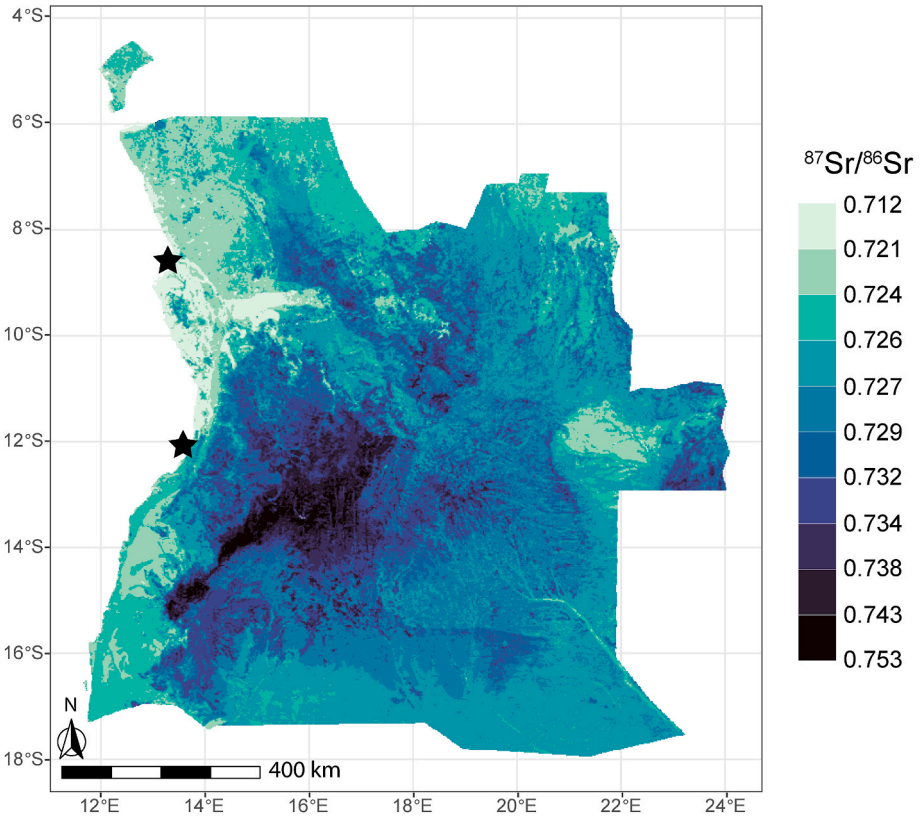

Fig. 2. $^{87}Sr/^{86}Sr$ isoscape of Angola using random forest regression model. The scale of $^{87}Sr/^{86}Sr$ is classified by Fisher-Jenks natural breaks that optimize the variance within and between classes (Slocum et al., 2008).

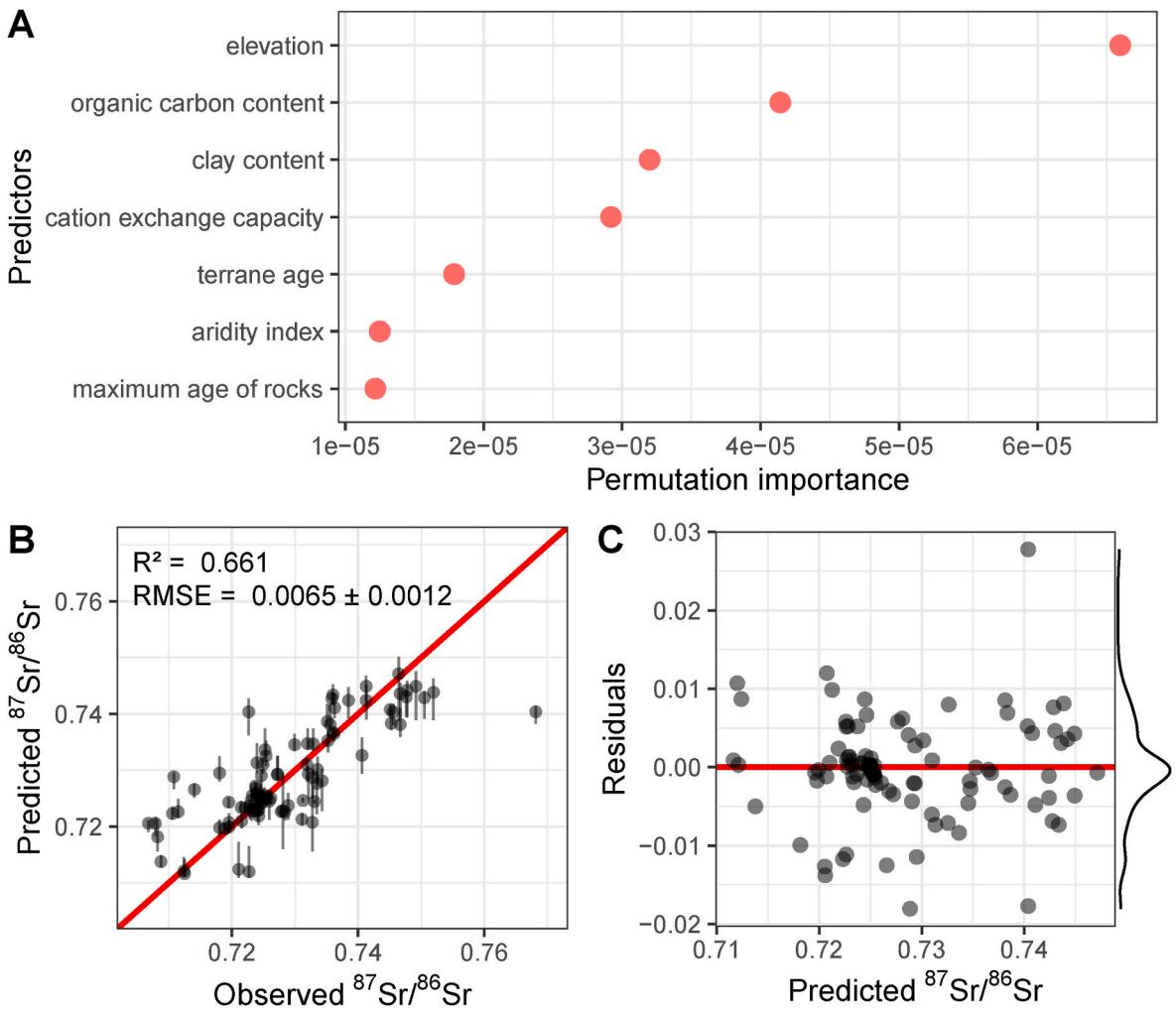

Fig. 3. Modeling results. **A.** Permutation importance for the random forest model using 7 variables (see Table 1). **B.** Predicted bioavailable $^{87}Sr/^{86}Sr$ vs observed bioavailable $^{87}Sr/^{86}Sr$ using the 5-fold cross-validation test. **C.** Residuals of the random forest regression model against predicted bioavailable $^{87}Sr/^{86}Sr$.

direct $^{87}Sr/^{86}Sr$ data, particularly at the edges of regions where categorical factors (e.g. lithology and land cover) change abruptly (Holt et al., 2021).

In Fig. 4D, the prediction performance for Angola is generally poor in Bataille et al. (2020), only explaining less than 1% of the variance of the observed ratios and showing a very large RMSE (0.0175), due to the absence of local bioavailable $^{87}Sr/^{86}Sr$ data in this global model. Particularly in the radiogenic $^{87}Sr/^{86}Sr$ regions of the Angola Block, the predicted $^{87}Sr/^{86}Sr$ ratios are much lower than the observed ratios. This indicates that although the machine learning has good prospects for generating Sr isoscapes, sampling on the ground is necessary in areas with very few empirical isotopic data when attempting to produce an accurate baseline map to address scientific questions.

3.4. *Implications for life histories during the transatlantic slave trade*

In light of our new Angola Sr isoscape presented above, we reinterpreted the published $^{87}Sr/^{86}Sr$ data of four selected individuals from four slave cemeteries with the aim to identify if these individuals could originate from Angola (Fig. 5).

Overall, individuals from these sites show very large variation in $^{87}Sr/^{86}Sr$ ratios ranging from 0.706 to 0.750, indicating they are of diverse geological and geographic origin (Fig. 5A). We used our novel Sr isoscape of Angola to map the probability of origin of four selected individuals with $^{87}Sr/^{86}Sr$ ratios higher than 0.730. The probability maps show that the possible origins of individuals with $^{87}Sr/^{86}Sr$ ratios of 0.73076 and 0.73433 are distributed across Angola (Fig. 5C and D, but see discussion of conflicting evidence below). We can be more specific with two individuals with $^{87}Sr/^{86}Sr$ ratios of 0.73912 and 0.74985, which can be assigned to more limited regions in central Angola (Fig. 5E and B). Based on ethno-linguistic evidence, it has been estimated that the origins of enslaved and deported Africans from Angola lied within a 200–300 km (max. 400 km) stretching along the Atlantic coast (Domingues da Silva, 2017), which may allow to further limit the most likely regions of individual origin.

However, when relying on $^{87}Sr/^{86}Sr$ data for such interpretations alone, it is important to consider that highly radiogenic $^{87}Sr/^{86}Sr$ ratios have also been reported for northern South Africa and Zimbabwe. We would argue, that first, such high ratios (>0.754) are more radiogenic than what has been found in human remains from African Diaspora contexts so far. Second, we can utilize historical data to eluate the likelihood that the enslaved individuals from African Diaspora contexts in the Americas may have originated from Angola, rather than from e.g. Zimbabwe. Zimbabwe lies farther east than historical evidence suggests that human trafficking routes leading to Atlantic ports extended. Some European slave ships did venture around the Cape of Good Hope to acquire captives in ports of southern East Africa, along the coast of modern Mozambique (and hence closer to Zimbabwe). However, such vessels were far fewer in number than ships taking on captives in Angola. More than ten times as many captives in the transatlantic slave trade embarked from West Central Africa (including Angola) and St. Helena (~5.7 Million) than from ports in southern East Africa, including

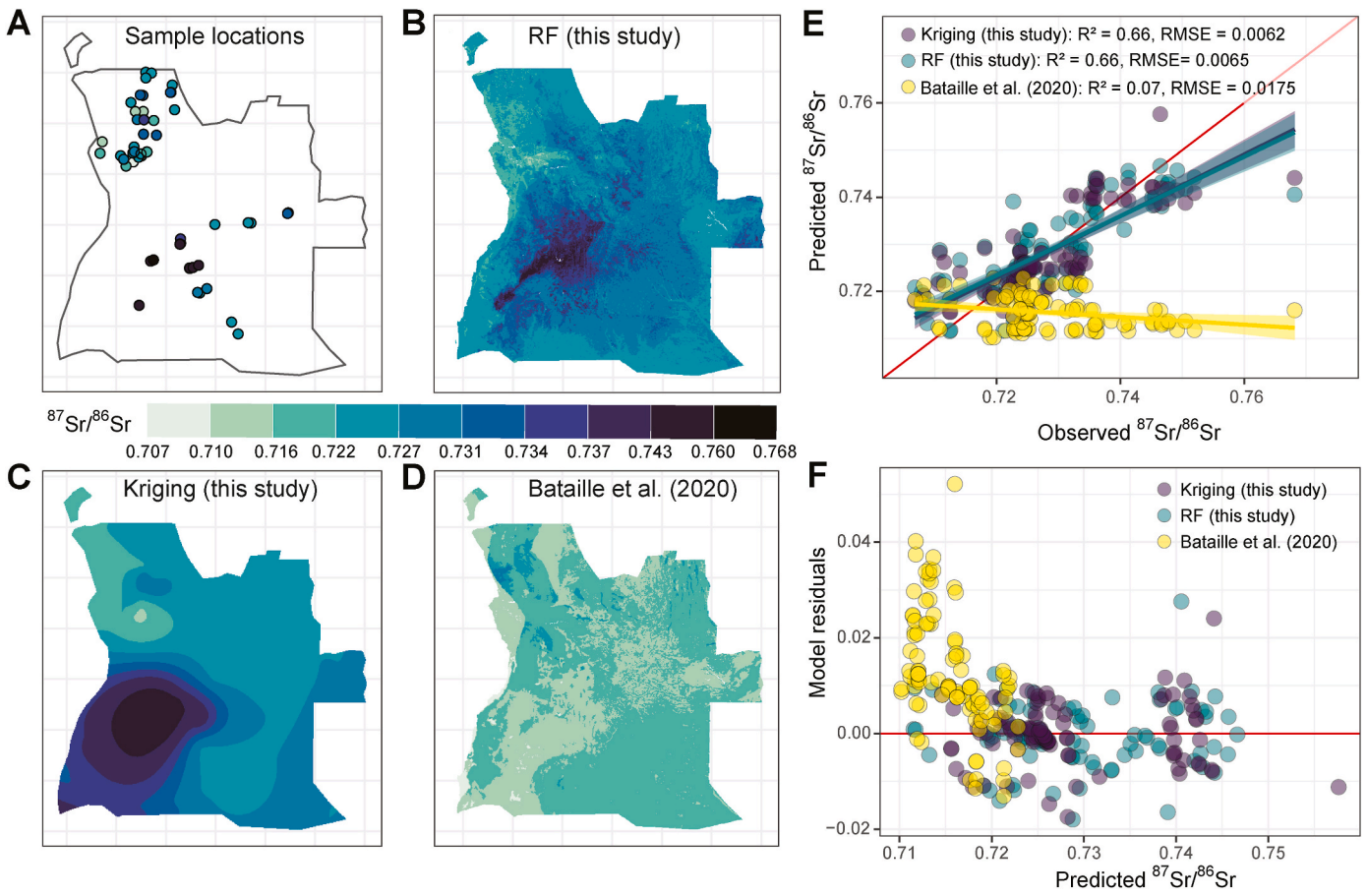

Fig. 4. The comparisons of different models mapping the Sr isoscape of Angola. **A.** Sample locations in this study. **B.** Random forest regression model in this study. **C.** Ordinary kriging interpolation using Angola samples. **D.** Bataille et al. (2020) global isoscape using random forest regression without environmental samples from Angola. **E.** Linear regressions between predicted (purple: results of cross-validation for the ordinary kriging, blue: results of cross-validation for the random forest from this study, yellow: extracted from global isoscape from Bataille et al. (2020)) and observed $^{87}Sr/^{86}Sr$ ratios among different models. **F.** Residuals of the models against predicted $^{87}Sr/^{86}Sr$ ratios.

the Indian Ocean islands (~542,000) as we can extract from the from the Slave Voyages Database (Trans-Atlantic Slave Trade Database, 2022; also discussed in Fleskes et al., 2023). Furthermore, southern East Africa only became relevant during the later phase of the transatlantic slave trade, after the U.S. and Great Britain abolished the transatlantic slave trade in 1808 (Trans-Atlantic, 2022). In Table 2 we summarize estimates from which regions enslaved Africans were abducted to the four broader destinations relevant for the burial sites discussed here, showing how predominant western Central Africa was during the slave trade of the 16th to the middle of the 19th century, in contrast to southern East Africa.

A community-based aDNA study on the Anson Street African Burial Ground in Charleston, suggested that none of the 18 tested individuals had distinguishable ancestry in southeastern Africa, well in line with aforementioned historic records (Fleskes et al., 2023). The results of this genetic investigation partly supports our interpretation that several individuals from Anson Street African Burial Ground had roots in what is now Angola, for other individuals, however, the novel genetic data contradicts our data interpretation. Two individuals, Ganda (CHS23) and Daba (CHS17), isotopically appear to come from Angola, with the probability of specific regional Angolan origins for Ganda shown in Fig. 5C, yet both of their genetic ancestry was clearly identified as West-African, with close genetic ties to e.g. Ghana and Côte d'Ivoire (Fleskes et al., 2023). According to our own yet unpublished data, there are serval regions dominated by ancient granites in western Côte d'Ivoire, southern Ghana, eastern Liberia and Guinea with bioavailable $^{87}Sr/^{86}Sr$ ratios ranging from 0.730 to 0.736 (Wang et al. in prep.), which match the $^{87}Sr/^{86}Sr$ ratios measured in the teeth of these two individuals. This clearly illustrates the need for Sr isoscapes for larger regions of Africa; work which is currently underway. Three other individuals (Banza/CHS01, Kuto/CHS04, Zimbu/CHS13) are clustering closely to Ganda and Daba in their respective $^{87}Sr/^{86}Sr$ ratios, but all three were shown to be of West-Central African descent, with genetic ties to modern populations in Angola, Cameroon and Gabon (Fleskes et al., 2023). In these individual cases, the genetic evidence matches our re-interpretation of the human $^{87}Sr/^{86}Sr$ data. The presence of West Africa individuals in North America is not surprising, but also the identification of Angolan individuals in colonial South Carolina's Anson Street Burial Ground via genetic and isotopic data, finds broad historic support. Prior to 1800, when this cemetery was in use, only two known vessels transported enslaved people directly from Angola to the British colonies of North America, and both of those went to Virginia, not South Carolina (Trans-Atlantic Slave Trade Database, 2022). Early in its development, however, South Carolina often relied on indirect deliveries of enslaved people from other American colonies. English and Dutch privateers also plundered Spanish and Portuguese vessels and settlements and sometimes stole enslaved people for delivery to North American colonies (O'Malley 2014). Such intra-American trafficking may explain the pathway of West-Central Africans finding their final resting place in South Carolina.

Further, the isotopic data from the Pretos Novos cemetery in Brazil suggest slightly larger numbers of individuals of possible Angolan origin (see Fig. 5A and B). This pattern fits well with historical data on the Atlantic slave trade and Portugal and Brazil's strong historical presence in Angolan human trafficking (Miller, 1988; Eltis and Richardson, 2010;

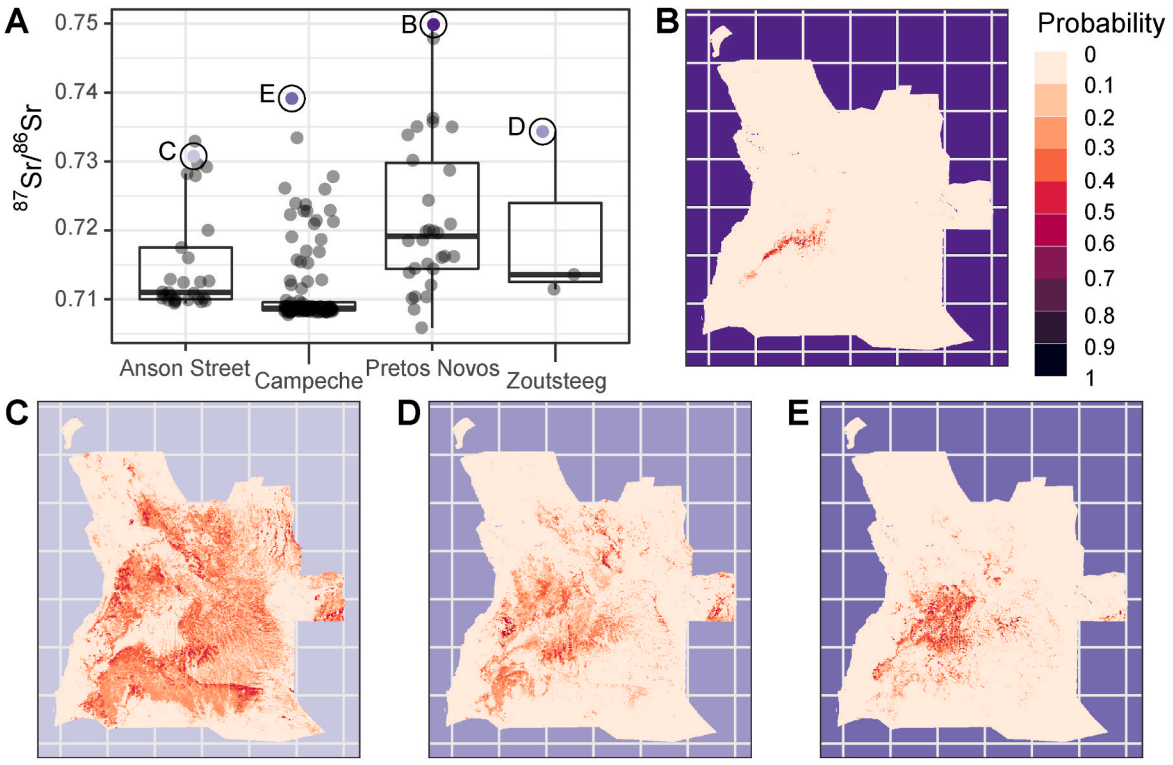

Fig. 5. Geographic assignment of origin for selected individuals. **A.** Previously published human enamel $^{87}Sr/^{86}Sr$ ratios from four slave cemeteries in the New World. **B.** Probability of origin for an individual with the $^{87}Sr/^{86}Sr$ ratio of 0.74985 from the Pretos Novos cemetery in Rio de Janeiro. **C.** Probability of origin for an individual with the $^{87}Sr/^{86}Sr$ ratio of 0.73076 from the Anson Street African Burial Ground in Charleston. **D.** Probability of origin for an individual with the $^{87}Sr/^{86}Sr$ ratio of 0.73433 from the Zoutsteeg area of Philipsburg. **E.** Probability of origin for an individual with the $^{87}Sr/^{86}Sr$ ratio of 0.73912 from the Campeche cemetery in Mexico.

Table 2
Transatlantic Slave Trade estimates between 1501 and 1866 for enslaved people embarking and disembarking at specific regions relevant for the four burial sites for which we re-evaluate the human $^{87}Sr/^{86}Sr$ data in this study (Trans-Atlantic Slave Trade Database, 2022; http://www.slavevoyages.org/estimates, last accessed 1/17/2023).

Burial site	City	Country	Disembarkation region	Embarkation region	
				West Central Africa & St. Helena	southern East Africa & Indian Ocean islands
Anson Street	Charleston	United States	Carolinas/Georgia	70,303	2297
Zoutsteeg	Philipsburg	Sint Maarten	Dutch Caribbean	69,272	597
Pretos Novos	Rio de Janeiro	Brazil	south-east Brazil	2,235,079	280,286
Campeche	Campeche	Mexico	Spanish Americas	635,594	114,748

Domingues da Silva, 2013). The lower proportion but still notable presence of individuals of possible Angolan origin in the Campeche burials from Mexico and Sint Maarten in the Dutch Caribbean also tracks well with historical understandings of the slave trade, since Portuguese traffickers were major suppliers of enslaved people to Spanish colonies, and the Dutch occupied the Angolan port of Luanda in the 1640s. According to historic records, both Mexico and the Dutch Caribbean had enslaved individuals arriving from Angola and other places before and during the period the cemeteries of Campeche and Zoutsteeg were active (Borucki et al., 2015).

3.5. Limitations and further directions

Although we are confident that this study provides useful environmental isotopic data and a novel Sr isoscape from an understudied region of Africa with considerable prehistoric and historic relevance, there are limitations to the study presented here.

One limitation of the random forest modeling is the inability of the model to extrapolate predictions outside of the range of the training dataset. This leads to poorer fit at the extremes (see Fig. 3B) and a reduced accuracy in low sampled regions. To mitigate those effects, we visually controlled that our sampling was representing the distribution of the different predictors throughout Angola. We feel confident that the majority of the chosen predictors are well represented within our (small) sampling. Given RF models are not able to reliably predict into regions without any previous sampling on the ground (Bataille et al., 2020), these limitations will persist until we start sampling underrepresented regions. Countless museums and other institutions house well curated, untreated and georeferenced organic materials from remote places around the world. We here demonstrate that sampling such existing collections, particularly herbarium material, can be incredibly useful in this context. Further isoscape studies might consider delving more deeply into checking the overlap of the parameter space between sampling and prediction location for example. Moreover, as emphasized by Bataille et al. (2020), improved resolution of potential predictors, particularly high-resolution geochemical and lithographic maps as well as empirical data on aerosol/dust deposition, will greatly help to improve the quality of future models and their predictions. Most of the variables used in isoscape modeling are themselves global predictions derived from models based on data generally sparsely representing the

African continent in particular. We are hopeful that the future leads to higher accuracy for both, African environmental data as modeling predictors and African environmental $^{87}Sr/^{86}Sr$ data itself.

Further, although parts of the geology of Angola appear to be indeed particularly old for West and western Central Africa, and our isoscape shows potential to identify the possible origins of enslaved people with $^{87}Sr/^{86}Sr$ ratios between 0.730 and 0.754, we are aware this assessment is based on the still very limited availability of $^{87}Sr/^{86}Sr$ data from any other region in western Central and Western Africa at this time. Similarly, any possible $^{87}Sr/^{86}Sr$ ratios higher than 0.754 could so far only be associated with parts of Zimbabwe or South Africa, the only regions in Africa for which such radiogenic bioavailable $^{87}Sr/^{86}Sr$ ratios have been described (Copeland et al., 2023; House et al., 2021).

Also, it is still very difficult to constrain the geographical origins of the vast number of enslaved Africans with lower $^{87}Sr/^{86}Sr$ ratios between 0.706 and 0.730 because the geographical area of this $^{87}Sr/^{86}Sr$ range spreads widely not only in coastal and northern Angola, but also many other parts of Africa. An extended Sr isoscape for all of subsaharan Africa based on environmental samples is currently in development (Wang et al. in prep), but will not alleviate this issue of reoccurring $^{87}Sr/^{86}Sr$ ratios across a vast continent. The way forward to gain a reliable forensic assessment of the provenience of enslaved Africans found across the globe is most likely the combination of various lines of isotopic, historic and genetic evidence. Pioneering community based research on the Anson Street African Burial Ground in Charleston leads by example here, by combining isotopic, genetic and historic evidence to identify individual African roots of the Anson Street Ancestors (Fleskes et al., 2021, 2023).

Future work on human remains should increasingly be informed by multiple lines of empirical evidence such as multiple isotope analysis (strontium, carbon, sulfur, oxygen, and nitrogen), ancient DNA, and when possible also historic or linguistic data to refine assessments of individual African origins. The same is true when we consider the use of this Angolan Sr isoscape for other lines of future research in which the provenance or movement of individuals is tracked, e.g. in African paleoanthropology (Copeland et al., 2011) and paleontology (Copeland et al., 2016; Lehmann et al., 2018), modern forensics of humans (Degryse et al., 2012) or endangered wildlife (Flockhart et al., 2015; Vlam et al., 2018) as well as animal ecology (Hobson, 1999; Reich et al., 2021).

4. Conclusions

This study presents the first draft of a bioavailable $^{87}Sr/^{86}Sr$ isoscape for Angola based on local samples and a random forest regression modeling approach, and illustrates the potential for using $^{87}Sr/^{86}Sr$ analysis in archaeological mobility research in this specific region. In particular, this study aims to provide novel information to answer critical questions regarding the origins of enslaved Africans during the transatlantic slave trade. The bioavailable $^{87}Sr/^{86}Sr$ ratios measured across Angola shows considerable variability in different geological units. The high ratios in the Angola Block in central Angola can be well distinguished from other regions in West and western Central Africa, providing indictors for interpreting the origins of high $^{87}Sr/^{86}Sr$ targets. This specificity will corroborate a strong correlation between the central region of Angola and the possible origin of enslaved individuals with the high $^{87}Sr/^{86}Sr$ ratios found in the context of the African Diaspora.

Our model incorporates local sampling into a machine learning framework, greatly improving the previous Angola map derived from a global $^{87}Sr/^{86}Sr$ isoscape prediction. This suggests that machine learning methods need to be combined with local sampling to improve the accuracy of local predictions. We anticipate that future work will continue to improve the predictive power of $^{87}Sr/^{86}Sr$ isoscapes though 1) increased density of sampling in the field covering yet underrepresented regions and 2) the availability of higher resolution geochemical maps as predictors for modeling.

Overall, our study lays a solid foundation for future provenance and mobility studies on the transatlantic and Atlantic slave trade as well as a wide range of research on ancient and modern human and animal mobility in archaeology, ecology and forensic studies.

Funding

This work was supported by the Webster Foundation. Fieldwork by M. Finckh & P. Meller was supported by the German Federal Ministry of Education and Research BMBF (Grant no. 01LG1201N).

Declaration of competing interest

The authors declare that they have no known competing financial interests or personal relationships that could have appeared to influence the work reported in this paper.

Acknowledgements

The spark to initiate this study was provided by Hannes Schroeder and Jason Laffoon and we are grateful for their inspiration to study $^{87}Sr/^{86}Sr$ variation in Angola. We thank Terry Blackburn and Gavin Piccione for assistance with isotope analysis in the W.M. Keck lab and Karen Dehn for logistical support. We thank Simon C. Brewer for clarifications on random forest modeling, as well as Pedro Dinis and Eduardo Garzanti for providing geological information of Angola. We are grateful for the constructive feedback from three anonymous reviewers, Clement Bataille and the editor. Plant sampling was carried out in collaboration with the Instituto Nacional da Biodiversidade a Areas de Conservação (INBAC) of the Ministério da Cultura, Turismo e Ambiente da República de Angola, the Direcção Provincial da Agricultura, Pecuária e Pescas of Uíge Province and Cuanza Norte Province, our partners at the Universidade Kimpa Vita and Instituto Superior de Ciencias de Educaão da Huila (ISCED-Huila) as well as the National Directorate of Agriculture, Lifestock and Forest of Angola.

Appendix A. Supplementary data

Supplementary data to this article can be found online at https://doi.org/10.1016/j.jas.2023.105775.

References

Allègre, C.J., Dupré, B., Négrel, P., Gaillardet, J., 1996. Sr-Nd-Pb isotope systematics in Amazon and Congo River systems: constraints about erosion processes. Chem. Geol. 131, 93–112. https://doi.org/10.1016/0009-2541(96)00028-9.

Bambi, A., Costanzo, A., Gonçalves, A., Melgarejo, J., 2012. Tracing the chemical evolution of primary pyrochlore from plutonic to volcanic carbonatites: the role of fluorine. Min. Mag. 76, 377–392. https://doi.org/10.1180/minmag.2012.076.2.07.

Barberena, R., Cardillo, M., Lucero, G., le Roux, P.J., Tessone, A., Llano, C., et al., 2021. Bioavailable strontium, human paleogeography, and migrations in the Southern Andes: A Machine Learning and GIS Approach. Front. Ecol. Evol. 9, 584325 https://doi.org/10.3389/fevo.2021.584325.

Barquera, R., Lamnidis, T.C., Lankapalli, A.K., Kocher, A., Hernández-Zaragoza, D.I., Nelson, E.A., et al., 2020. Origin and health status of first-generation Africans from early colonial Mexico. Curr. Biol. 30, 2078–2091. https://doi.org/10.1016/j.cub.2020.04.002.

Bastos, M.Q.R., Santos, R.V., de Souza, M., Rodrigues-Carvalho, C., Tykot, R.H., Cook, D. C., et al., 2016. Isotopic study of geographic origins and diet of enslaved Africans buried in two Brazilian cemeteries. J. Archaeol. Sci. 70, 82–90. https://doi.org/10.1016/j.jas.2016.04.020.

Bataille, C.P., Crowley, B.E., Wooller, M.J., Bowen, G.J., 2020. Advances in global bioavailable strontium isoscapes. Palaeogeogr. Palaeoclimatol. Palaeoecol. 555, 109849 https://doi.org/10.1016/j.palaeo.2020.109849.

Bataille, C.P., von Holstein, I.C.C., Laffoon, J.E., Willmes, M., Liu, X.M., Davies, G.R., 2018. A bioavailable strontium isoscape for Western Europe: A machine learning approach. PloS one 13, e0197386. https://doi.org/10.1371/journal.pone.0197386.

Benito, M., 2021. spatialRF: Easy spatial regression with random forest. R package version 1.1.0. https://blasbenito.github.io/spatialRF/.

Bentley, R.A., 2006. Strontium isotopes from the earth to the archaeological skeleton: a review. J. Archaeol. Method Theory 13, 135–187. https://doi.org/10.1007/s10816-006-9009-x.

Borucki, A., Eltis, D., Wheat, D., 2015. Atlantic history and the slave trade to Spanish America. Am. Hist. Rev. 120, 433–461. https://doi.org/10.1093/ahr/120.2.433.
Breiman, L., 2001. Random Forests. Mach. Learn. 45, 5–32. https://doi.org/10.1023/A:1010933404324.
Capo, R.C., Stewart, B.W., Chadwick, O.A., 1998. Strontium isotopes as tracers of ecosystem processes: theory and methods. Geoderma 82, 197–225. https://doi.org/10.1016/s0016-7061(97)00102-x.
Chaboureau, A.C., Guillocheau, F., Robin, C., Rohais, S., Moulin, M., Aslanian, D., 2013. Paleogeographic evolution of the central segment of the South Atlantic during Early Cretaceous times: Paleotopographic and geodynamic implications. Tectonophysics 604, 191–223. https://doi.org/10.1016/j.tecto.2012.08.025.
Copeland, S.R., Cawthra, H.C., Fisher, E.C., Lee-Thorp, J.A., Cowling, R.M., le Roux, P.J., et al., 2016. Strontium isotope investigation of ungulate movement patterns on the Pleistocene Paleo-Agulhas Plain of the Greater Cape Floristic Region, South Africa. Quat. Sci. Rev. 141, 65–84. https://doi.org/10.1016/j.quascirev.2016.04.002.
Copeland, S.R., Grimes, V., Neveling, J., Lee-Thorp, J.A., Grine, F., Yang, Z.P., et al., 2023. Isotopic evidence for the geographic origin, movement and diet of the Hofmeyr individual. In: Grine, F.E. (Ed.), Hofmeyr. Vertebrate Paleobiology and Paleoanthropology. Springer Nature, Switzerland, Cham, pp. 47–71.
Copeland, S.R., Sponheimer, M., de Ruiter, D.J., Lee-Thorp, J.A., Codron, D., le Roux, P. J., et al., 2011. Strontium isotope evidence for landscape use by early hominins. Nature 474 (7349), 76–78. https://doi.org/10.1038/nature10149.
Copeland, S.R., Sponheimer, M., le Roux, P.J., Grimes, V., Lee-Thorp, J.A., de Ruiter, D. J., et al., 2008. Strontium isotope ratios ($^{87}Sr/^{86}Sr$) of tooth enamel: a comparison of solution and laser ablation multicollector inductively coupled plasma mass spectrometry methods. Rapid Commun. Mass Spectrom. 22, 3187–3194. https://doi.org/10.1002/rcm.3717.
Crowley, B.E., Miller, J.H., Bataille, C.P., 2017. Strontium isotopes ($^{87}Sr/^{86}Sr$) in terrestrial ecological and palaeoecological research: empirical efforts and recent advances in continental-scale models. Biol. Rev. 92, 43–59. https://doi.org/10.1111/brv.12217.
De Carvalho, H., Tassinari, C., Alves, P., Guimarães, F., Simões, M., 2000. Geochronological review of the Precambrian in western Angola: links with Brazil. J. Afr. Earth Sci. 31, 383–402. https://doi.org/10.1016/S0899-5362(00)00095-6.
de Matos, D., 2015. Review of the Stone Age archaeology in southwestern Angola. Africana Studia 24, 33–38.
de Matos, D., Martins, A.C., Senna-Martinez, J.C., Pinto, I., Coelho, A.G., Ferreira, S.S., et al., 2021. Review of archaeological research in Angola. Afr. Archaeol. Rev. 38, 319–344. https://doi.org/10.1007/s10437-020-09420-8.
de Matos, D., Pereira, T., 2020. Middle Stone Age lithic assemblages from Leba Cave (Southwest Angola). J. Archaeol. Sci.: Rep. 32, 102413 https://doi.org/10.1016/j.jasrep.2020.102413.
De Waele, B., Johnson, S.P., Pisarevsky, S.A., 2008. Palaeoproterozoic to Neoproterozoic growth and evolution of the eastern Congo Craton: Its role in the Rodinia puzzle. Precambrian Res 160, 127–141. https://doi.org/10.1016/j.precamres.2007.04.020.
Degryse, P., De Muynck, D., Delporte, S., Boyen, S., Jadoul, L., De Winne, J., et al., 2012. Strontium isotopic analysis as an experimental auxiliary technique in forensic identification of human remains. Anal. Methods 4, 2674–2679. https://doi.org/10.1039/C2AY25035G.
Deniel, C., Pin, C., 2001. Single-stage method for the simultaneous isolation of lead and strontium from silicate samples for isotopic measurements. Anal. Chim. Acta. 426, 95–103. https://doi.org/10.1016/S0003-2670(00)01185-5.
Dinis, P., Garzanti, E., Vermeesch, P., Huvi, J., 2017. Climatic zonation and weathering control on sediment composition (Angola). Chem. Geol. 467, 110–121. https://doi.org/10.1016/j.chemgeo.2017.07.030.
Domingues da Silva, D.B., 2013. The Atlantic Slave Trade from Angola: A port-by-port estimate of slaves embarked, 1701–1867. Int. J. Afr. Hist. Stud. 46, 105–122.
Domingues da Silva, D.B., 2017. The Atlantic slave trade from West Central Africa, 1780–1867. Cambridge University Press, Cambridge.
Dominy, N.J., Ikram, S., Moritz, G.L., Wheatley, P.V., Christensen, J.N., Chipman, J.W., et al., 2020. Mummified baboons reveal the far reach of early Egyptian mariners. Elife 9, e60860. https://doi.org/10.7554/eLife.60860.
Eltis, D., Richardson, D., 2010. Atlas of the Transatlantic Slave Trade. Yale University Press, New Haven.
Ericson, J.E., 1985. Strontium isotope characterization in the study of prehistoric human ecology. J. Hum. Evol. 14, 503–514. https://doi.org/10.1016/S0047-2484(85)80029-4.
Fleskes, R.E., Ofunniyin, A.A., Gilmore, J.K., Poplin, E., Abel, S.M., Bueschgen, W.D., et al., 2021. Ancestry, health, and lived experiences of enslaved Africans in 18th century Charleston: An osteobiographical analysis. Am. J. Phys. Anthropol. 175, 3–24. https://doi.org/10.1002/ajpa.24149.
Fleskes, R.E., Cabana, G.S., Gilmore, J.K., Juarez, C., Karcher, E., Oubré, L., et al., 2023. Community-engaged ancient DNA project reveals diverse origins of 18th-century African descendants in Charleston, South Carolina. Proc. Natl Acad. Sci. USA 120, e2201620120. https://doi.org/10.1073/pnas.2201620120.
Flockhart, D.T.T., Kyser, T.K., Chipley, D., Miller, N.G., Norris, D.R., 2015. Experimental evidence shows no fractionation of strontium isotopes ($^{87}Sr/^{86}Sr$) among soil, plants, and herbivores: implications for tracking wildlife and forensic science. Isot. Environ. Health Stud. 51, 372–381. https://doi.org/10.1080/10256016.2015.1021345.
Fowler, K.D., Yang, P., Halden, N.M., 2020. The provisioning of nineteenth century Zulu capitals, South Africa: Insights from strontium isotope analysis of cattle remains. J. Archaeol. Sci.: Rep. 31, 102306 https://doi.org/10.1016/j.jasrep.2020.102306.
Fricke, F., Laffoon, J., Espersen, R., 2021. Unforgotten: The osteobiography of an enslaved woman and child from 18th century Saba. J. Archaeol. Sci.: Rep. 36, 102838 https://doi.org/10.1016/j.jasrep.2021.102838.
Garzanti, E., Dinis, P., Vermeesch, P., Andò, S., Hahn, A., Huvi, J., et al., 2018. Dynamic uplift, recycling, and climate control on the petrology of passive-margin sand (Angola). Sediment. Geol. 375, 86–104. https://doi.org/10.1016/j.sedgeo.2017.12.009.
Genuer, R., Poggi, J., Tuleau-Malot, C., 2019. VSURF: variable selection using random forests. R package version 1.1. 0. https://CRAN.R-project.org/package=VSURF.
Gilbert, C.C., McGraw, W.S., Delson, E., 2009. Brief communication: Plio-Pleistocene eagle predation on fossil cercopithecids from the Humpata Plateau, southern Angola. Am. J. Phys. Anthropol. 139, 421–429. https://doi.org/10.1002/ajpa.21004.
Goodman, A., Jones, J., Reid, J., Mack, M., Blakey, M.L., Amarasiriwardena, D., et al., 2004. Isotopic and elemental chemistry of teeth: implications for places of birth, forced migration patterns, nutritional status, and pollution. The New York African burial ground skeletal biology final report 1, 216–265.
Gregorutti, B., Michel, B., Saint-Pierre, P., 2017. Correlation and variable importance in random forests. Stat. Comput. 27, 659–678. https://doi.org/10.1007/s11222-016-9646-1.
Haddon, I.G., McCarthy, T.S., 2005. The Mesozoic–Cenozoic interior sag basins of Central Africa: The Late-Cretaceous–Cenozoic Kalahari and Okavango basins. J. Afr. Earth Sci. 43, 316–333. https://doi.org/10.1016/j.jafrearsci.2005.07.008.
Hajj, F., Poszwa, A., Bouchez, J., Guérold, F., 2017. Radiogenic and "stable" strontium isotopes in provenance studies: A review and first results on archaeological wood from shipwrecks. J. Archaeol. Sci. 86, 24–49. https://doi.org/10.1016/j.jas.2017.09.005.
Hartmann, J., Moosdorf, N., 2012. The new global lithological map database GLiM: A representation of rock properties at the Earth surface. Geochem. Geophy. Geosyst. 13, Q12004.
Hengl, T., Mendes de Jesus, J., Heuvelink, G.B.M., Ruiperez Gonzalez, M., Kilibarda, M., Blagotić, A., et al., 2017. SoilGrids250m: Global gridded soil information based on machine learning. PloS one 12, e0169748. https://doi.org/10.1371/journal.pone.0169748.
Hobson, K., 1999. Tracing origins and migration of wildlife using stable isotopes: a review. Oecologia 120, 314–326. https://doi.org/10.1007/s004420050865.
Holt, E., Evans, J.A., Madgwick, R., 2021. Strontium ($^{87}Sr/^{86}Sr$) mapping: A critical review of methods and approaches. Earth-Sci. Rev. 216, 103593 https://doi.org/10.1016/j.earscirev.2021.103593.
Hoogewerff, J.A., Reimann, C., Ueckermann, H., Frei, R., Frei, K.M., van Aswegen, T., et al., 2019. Bioavailable $^{87}Sr/^{86}Sr$ in European soils: A baseline for provenancing studies. Sci. Total Environ. 672, 1033–1044. https://doi.org/10.1016/j.scitotenv.2019.03.387.
House, M., Sealy, J., Chirikure, S., Le Roux, P., 2021. Investigating Cattle Procurement at Great Zimbabwe Using $^{87}Sr/^{86}Sr$. J. Afr. Archaeol. 19, 146–158.
Janzen, A., Bataille, C., Copeland, S.R., Quinn, R.L., Ambrose, S.H., Reed, D., et al., 2020. Spatial variation in bioavailable strontium isotope ratios ($^{87}Sr/^{86}Sr$) in Kenya and northern Tanzania: Implications for ecology, paleoanthropology, and archaeology. Palaeogeogr. Palaeoclimatol. Palaeoecol. 560, 109957 https://doi.org/10.1016/j.palaeo.2020.109957.
Jarvis, A., Reuter, A., Nelson, A., Guevara, E., 2008. Hole-filled SRTM for the globe Version 4, available from the CGIAR-CSI SRTM 90m Database. CGIAR CSI Consort. Spat. Inf. 1-9.
Kramer, R.T., Kinaston, R.L., Holder, P.W., Armstrong, K.F., King, C.L., Sipple, W.D.K., et al., 2022. A bioavailable strontium ($^{87}Sr/^{86}Sr$) isoscape for Aotearoa New Zealand: Implications for food forensics and biosecurity. PloS one 17, e0264458. https://doi.org/10.1371/journal.pone.0264458.
Laffoon, J.E., Espersen, R., Mickleburgh, H.L., 2018. The life history of an enslaved African: Multiple isotope evidence for forced childhood migration from Africa to the Caribbean and associated dietary change. Archaeometry 60, 350–365. https://doi.org/10.1111/arcm.12354.
Lebatard, A.-E., Bourlès, D.L., Braucher, R., 2019. Absolute dating of an Early Paleolithic site in Western Africa based on the radioactive decay of in situ-produced 10Be and 26Al. Nucl. Instrum. Methods in Phys. Res. B: Beam Interact. Mater. At. 456, 169–179. https://doi.org/10.1016/j.nimb.2019.05.052.
Lehmann, S.B., Levin, N.E., Braun, D.R., Stynder, D.D., Zhu, M., Le Roux, P.J., et al., 2018. Environmental and ecological implications of strontium isotope ratios in mid-Pleistocene fossil teeth from Elandsfontein, South Africa. Palaeogeogr. Palaeoclimatol. Palaeoecol. 490, 84–94. https://doi.org/10.1016/j.palaeo.2017.10.008.
Lovejoy, P.E., 2012. Transformations in slavery: a history of slavery in Africa, third ed. Cambridge University Press, Cambridge.
Lovejoy, P.E., Richardson, D., 1995. Competing markets for male and female slaves: Prices in the interior of West Africa, 1780-1850. Int. J. Afr. Hist. Stud. 28, 261–293. https://doi.org/10.2307/221615.
Lugli, F., Cipriani, A., Bruno, L., Ronchetti, F., Cavazzuti, C., Benazzi, S., 2022. A strontium isoscape of Italy for provenance studies. Chem. Geol. 587, 120624 https://doi.org/10.1016/j.chemgeo.2021.120624.
Manning, P., 1982. Slavery, colonialism and economic growth in Dahomey, 1640–1960. Cambridge University Press, Cambridge.
Miller, J.C., 1988. Way of death: merchant capitalism and the Angolan slave trade, 1730–1830. University of Wisconsin Press, Madison.
Mooney, W.D., Laske, G., Masters, T.G., 1998. CRUST 5.1: a global crustal model at 5° × 5. J. Geophys. Res. Solid Earth 103, 727–747. https://doi.org/10.1029/97JB02122.
Négrel, P., Allègre, C.J., Dupré, B., Lewin, E., 1993. Erosion sources determined by inversion of major and trace element ratios and strontium isotopic ratios in river water: the Congo Basin case. Earth Planet. Sci. Lett. 120, 59–76. https://doi.org/10.1016/0012-821X(93)90023-3.
O'Malley, G.E., 2014. Final Passages: The Intercolonial Slave Trade of British America, 1619-1807. University of North Carolina Press, Chapel Hill, NC.

Palmer, M., Edmond, J., 1989. The strontium isotope budget of the modern ocean. Earth Planet. Sci. Lett. 92, 11–26. https://doi.org/10.1016/0012-821X(89)90017-4.
Price, T.D., Burton, J.H., Bentley, R.A., 2002. The characterization of biologically available strontium isotope ratios for the study of prehistoric migration. Archaeometry 44, 117–135. https://doi.org/10.1111/1475-4754.00047.
Price, T.D., Burton, J.H., Cucina, A., Zabala, P., Frei, R., Tykot, R.H., et al., 2012. Isotopic studies of human skeletal remains from a sixteenth to seventeenth century AD churchyard in Campeche, Mexico: Diet, place of origin, and age. Curr. Anthropol. 53, 396–433. https://doi.org/10.1086/666492.
Price, T.D., Tiesler, V., Burton, J.H., 2006. Early African Diaspora in colonial Campeche, Mexico: strontium isotopic evidence. Am. J. Phys. Anthropol. 130, 485–490. https://doi.org/10.1002/ajpa.20390.
Pye, K., 2004. Isotope and trace element analysis of human teeth and bones for forensic purposes. Geol. Soc. Lond. Spec. Publ. 232, 215–236. https://doi.org/10.1144/GSL.SP.2004.232.01.2.
Quinn, R.L., Warnasch, S.C., Watson, M., Godfrey, L., Setera, J.B., VanTongeren, J., et al., 2020. Biogeochemical evidence for residence, diet, and health of the Woman in the Iron Coffin (Queens, New York City). Int. J. Osteoarchaeol. 30, 225–235. https://doi.org/10.1002/oa.2850.
Reich, M.S., Flockhart, D.T., Norris, D.R., Hu, L., Bataille, C.P., 2021. Continuous-surface geographic assignment of migratory animals using strontium isotopes: A case study with monarch butterflies. Methods Ecol. Evol. 12, 2445–2457. https://doi.org/10.1111/2041-210X.13707.
Schroeder, H., Haviser, J.B., Price, T.D., 2014. The Zoutsteeg three: Three new cases of African types of dental modification from Saint Martin, Dutch Caribbean. Int. J. Osteoarchaeol. 24, 688–696. https://doi.org/10.1002/oa.2253.
Schroeder, H., O'Connell, T.C., Evans, J.A., Shuler, K.A., Hedges, R.E., 2009. Trans-Atlantic slavery: isotopic evidence for forced migration to Barbados. Am. J. Phys. Anthropol. 139, 547–557. https://doi.org/10.1002/ajpa.21019.
Serna, A., Prates, L., Mange, E., Salazar-García, D.C., Bataille, C.P., 2020. Implications for paleomobility studies of the effects of quaternary volcanism on bioavailable strontium: A test case in North Patagonia (Argentina). J. Archaeol. Sci. 121, 105198 https://doi.org/10.1016/j.jas.2020.105198.
Sillen, A., Hall, G., Richardson, S., Armstrong, R., 1998. $^{87}Sr/^{86}Sr$ ratios in modern and fossil food-webs of the Sterkfontein Valley: implications for early hominid habitat preference. Geochim. Cosmochim. Acta 62, 2463–2473. https://doi.org/10.1016/S0016-7037(98)00182-3.
Slocum, T.A., McMaster, R.B., Kessler, F., Howard, H.H., 2008. Thematic Cartography and Visualization, third ed. Prentice-Hall, Upper Saddle River, NJ.
Slovak, N.M., Paytan, A., 2012. Applications of Sr isotopes in archaeology. In: Baskaran, M. (Ed.), Handbook of Environmental Isotope Geochemistry: Vol I. Springer Berlin Heidelberg, Berlin, Heidelberg, pp. 743–768.
Smith-Guzmán, N.E., Rivera-Sandoval, J., Knipper, C., Sánchez Arias, G.A., 2020. Intentional dental modification in Panamá: New support for a late introduction of African origin. J. Anthropol. Archaeol. 60, 101226 https://doi.org/10.1016/j.jaa.2020.101226.
Thiéblement, D., Liégeois, J.-P., Fernandez-Alonso, M., , Ouabadi, Le Gall, A., B., Maury, R., et al., 2016. Geological map of Africa GIS database (Scale 1: 10 000 000).
Thornton, J., 1998. Africa and Africans in the Making of the Atlantic World, second ed. Cambridge University Press, Cambridge, pp. 1400–1800.
Trans-Atlantic Slave Trade Database, 2022. http://www.slavevoyages.org/estimates/XhJjAgtE. last accessed 1/13/2023.
Viers, J., Dupré, B., Braun, J.-J., Deberdt, S., Angeletti, B., Ngoupayou, J.N., et al., 2000. Major and trace element abundances, and strontium isotopes in the Nyong basin rivers (Cameroon): constraints on chemical weathering processes and elements transport mechanisms in humid tropical environments. Chem. Geol. 169, 211–241. https://doi.org/10.1016/S0009-2541(00)00298-9.
Vlam, M., de Groot, G.A., Boom, A., Copini, P., Laros, I., Veldhuijzen, K., et al., 2018. Developing forensic tools for an African timber: Regional origin is revealed by genetic characteristics, but not by isotopic signature. Biol. Conserv. 220, 262–271. https://doi.org/10.1016/j.biocon.2018.01.031.
Vogel, J.C., Eglington, B., Auret, J.M., 1990. Isotope fingerprints in elephant bone and ivory. Nature 346, 747–749. https://doi.org/10.1038/346747a0.
Wang, X., Tang, Z., 2020. The first large-scale bioavailable Sr isotope map of China and its implication for provenance studies. Earth-Sci. Rev. 210, 103353 https://doi.org/10.1016/j.earscirev.2020.103353.
Wang, X., Bocksberger, G., Agbor, A., Angedakin, S., Aubert, F., Ayimisin, Ayuk, et al., 2023. The first draft of a Pan African strontium isoscape with implications for historic and wildlife forensics (in preperation). Manuscript in preparation, January 2023.
Wright, M.N., Ziegler, A., König, I.R., 2016. Do little interactions get lost in dark random forests? BMC Bioinf 17, 145. https://doi.org/10.1186/s12859-016-0995-8.
Zomer, R.J., Trabucco, A., Bossio, D.A., Verchot, L.V., 2008. Climate change mitigation: A spatial analysis of global land suitability for clean development mechanism afforestation and reforestation. Agr. Ecosyst. & Environ. 126, 67–80. https://doi.org/10.1016/j.agee.2008.01.014.